CHEMISTRY OF MATERIALS

VOLUME 14, NUMBER 2 FEBRUARY 2002

Communications

WS_2 Nanotube Bundles and Foils

R. Rosentsveig,† A. Margolin,† Y. Feldman,‡ R. Popovitz-Biro,† and R. Tenne*,†

Department of Materials and Interfaces and Unit of Chemical Services, Weizmann Institute of Science, Rehovot 76100, Israel

Received July 24, 2001
Revised Manuscript Received November 13, 2001

WS_2 nanotubes and fullerene-like nanoparticles (denoted *IF*) were first observed by hydrosulfurization of a very thin film of tungsten.[1] Subsequently, *IF*-MoS_2[2] and the respective selenides[3] were reported. Recently, bundles of very long single-wall MoS_2 nanotubes 9.6 Å in diameter were prepared.[4] Furthermore, it was reported that multiwall nanotubes of many of the layered metal dichalcogenides could be prepared by the thermal decomposition of the respective ammonium thio-metalate precursor.[5] WS_2 nanotubes were prepared from a tungsten-oxide precursor by a two-step reaction[6,7] and their growth mechanism has been studied to some extent. MS_2 nanotubes are expected to reveal many interesting electronic and optical properties.[8−10] In the present work we use a fluidized-bed reactor (FBR) to prepare many grams of multiwall WS_2 nanotubes in a one-step reaction. A similar FBR has been previously used for the synthesis of fullerene-like WS_2 nanoparticles, but under somewhat different working parameters (lower feed rate of the WO_3 powder and a smaller rate of H_2S gas flow).[11] The very long nanotubes (few hundreds of micrometers) tend to form bundles, probably in the gaseous atmosphere of the FBR. However, a portion of the nanotubes was found to stick to the quartz wall of the reactor and self-assemble into a very thin foil, which upon detachment from the wall is separated into a few centimeter long ribbons. Some further insight into the growth mechanism of the nanotubes and the ribbons (bundles) is forwarded, too, in this report.

For the sake of these experiments, a FBR made of quartz glass was constructed. In this reactor WO_3 nanoparticles are fed (60−70 mg/min) from the top, which is facilitated by N_2 gas flow (60 mL/min). A mixture of gases consisting of H_2S (5−12 mL/min) and H_2(5%)/N_2(95%) (60−120 mL/min) flows from below, keeping the powder aloft. A temperature profile of between 800 and 840 °C is maintained along the 60-cm-long reactor. The powder is collected on a porous ceramic filter.

Once the reaction is completed, the reactor is allowed to cool down. The powder, which is collected on the

* To whom correspondence should be addressed.
† Department of Materials and Interfaces.
‡ Unit of Chemical Services.

(1) Tenne, R.; Margulis, L.; Genut M.; Hodes, G. *Nature* **1992**, *360*, 444.
(2) (a) Margulis, L.; Salitra, G.; Talianker, M.; Tenne, R. *Nature* **1993**, *365*, 113. (b) Feldman, Y.; Wasserman, E.; Srolovitz, D.; Tenne, R. *Science* **1995**, *267*, 222.
(3) Hershfinkel, M.; Gheber, L. A.; Volterra, V.; Hutchison, J. L.; Margulis, L.; Tenne, R. *J. Am. Chem. Soc.* **1994**, *116*, 1914.
(4) Remskar, M.; Mrzel, A.; Skraba, Z.; Jesih, A.; Ceh, M.; Demsar, J.; Stadelmann, P.; Lévy, F.; Mihailovic, D. *Science* **2001**, *292*, 479.
(5) Nath, M.; Rao, C. N. R. *J. Am. Chem. Soc.* **2001**, *123*, 4841.
(6) (a) Rothschild, A.; Frey, G. L.; Homyonfer, M.; Tenne, R.; Rappaport, M. *Mater. Res. Innovat.* **1999**, *3*, 145. (b) Rothschild, A.; Sloan, J.; Tenne, R. *J. Am. Chem. Soc.* **2000**, *122*, 5169.
(7) Zhu, Y. Q.; Hsu, W. K.; Grobert, N.; Chang, B. H.; Terrones, M.; Terrones, H.; Kroto, H. W.; Walton, D. R. M. *Chem. Mater.* **2000**, *12*, 1190.
(8) Seifert, G.; Terrones, H.; Terrones, M.; Jungnickel, G.; Frauenheim, T. *Phys. Rev. Lett.* **2000**, *85*, 146.
(9) Seifert, G.; Terrones, H.; Terrones, M.; Frauenheim, T. *Solid State Commun.* **2000**, *115*, 635.
(10) Kociak, M.; Stephan, O.; Henrard, L.; Charbois, V.; Rothschild, A.; Tenne, R.; Colliex, C. *Phys. Rev. Lett.* **2001**, *87*, 5501.
(11) Feldman, Y.; Zak, A.; Popovitz-Biro, R.; Tenne, R. *Solid State Sci.* **2000**, *2*, 663.

10.1021/cm010630f CCC: $22.00
Published on Web 02/01/2002

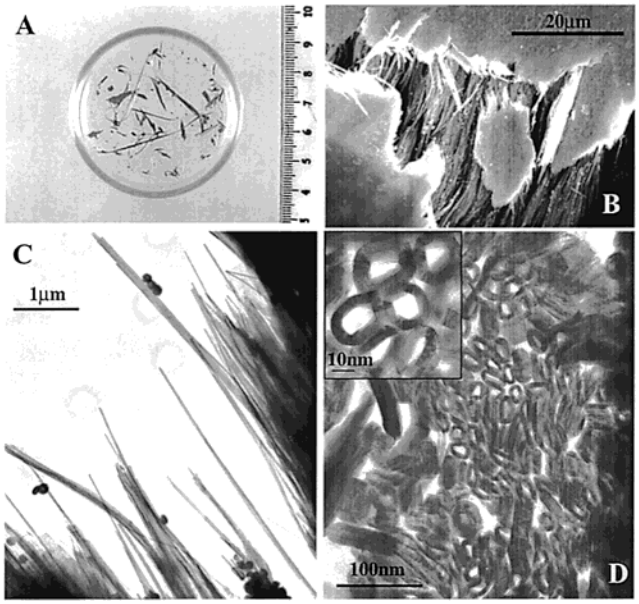

Figure 1. WS_2 ribbons inspected by a number of microscopy techniques: (a) optical microscopy of a group of WS_2 ribbons, obtained during the detachment of the foil from the reactor wall; (b) scanning electron microscopy of a deliberately broken ribbon showing the nanotubes protruding from the feasure area and the shiny WS_2 film obtained by fusion of the nanotubes on the reactor wall; (c) TEM image of the feasured ribbon; (d) a cross section of the ribbon obtained through microtomy of an embedded ribbon. In the inset a magnified TEM picture of the cross-sectioned nanotubes shows their lattice image.

porous ceramic filters, is examined by an optical microscope. Some 20 experiments were carried out in this series. In each experiment, 3−20 g of the *IF* powder was obtained after a few hours of experiment. In all but 3 experiments, long WS_2 nanotubes were found in substantial amounts (<10%). In a few cases ≈10-cm-long and a few millimeter thick wires consisting of nanotubes were obtained within the reactor. In other cases the powder of the fullerene-like WS_2 nanoparticles was mixed with very long WS_2 nanotubes or typically 1-cm-long bundles, which could be easily separated from the spherical nanoparticles using sieves of various meshes. In two cases, a very thin foil a few centimeters long and wide was found to stick to the quartz wall of the reactor. The side in contact with the tubular reactor exhibited a metallic luster, typical of the luster of the van der Waals surface of lamellar platelets of WS_2. On the other hand, the inner surface of the ribbon scatters the incident light and appears to the naked eye gray mat. Upon lifting the foil from the wall, it separated into very long ribbons 1−2-mm wide.

Figure 1a shows an optical microscope image of the WS_2 nanotube ribbons. Figure 1b shows a scanning electron microscope (SEM) picture of a fissured ribbon. Clearly, a large number of nanotubes are protruding from the feasure. A smooth film, which endows the ribbon with its metallic luster, coats the ribbon. Energy-dispersive analysis (EDS) of the sample showed that it consists of tungsten and sulfur, at a ratio of 1:2. The core of the ribbon consists of well-aligned nanotubes. Transmission electron microcopy (TEM) analysis (Figure 1c) showed long and uniform nanotubes, which are mostly 4−7-layers thick. To further analyze the structure of the ribbons, one of the ribbons was embedded in a polymer matrix and subsequently microtomed. Unfortunately, soaking the ribbon in the monomer suspension, before cross-linking, led to its partial swelling. Consequently, the nanotubes at the edges were loosened from the ribbon core. Perhaps as a result of the mechanical force exerted by the diamond knife of the microtome, the loosened bundles led to the outer nanotubes to tilt (left side of Figure 1d). Nonetheless, the core of the ribbon reveals clearly the section of well-aligned nanotubes. The observed nanotubes are somewhat squashed, so that their circular cross section was distorted. This deformation can be attributed to either the packing of the nanotubes in the bundle, to the contraction of the polymer during the embedding procedure, or to the diamond knife itself. The inset shows a lattice image of a few microtomed nanotubes. One can also notice fused and collapsed nanotubes on the right-hand side of the ribbon (Figure 1d). These collapsed nanotubes are making the shiny coating of the ribbon, which is attached to the quartz tube wall and are clearly evident in the SEM picture (Figure 1b). Unfortunately, the nanotubes in the ribbon cannot be easily isolated without rupturing them, and consequently it was impossible to determine their length or study their structure in great detail. It is believed that the nanotubes, which grow in the gas phase as oxide nanowhiskers coated by a few sulfide layers, each,[6] accumulate gradually on the quartz wall and form a foil (ribbon). The van der Waals interaction between the tubes leads to their almost perfect alignment. This packing mode of the nanotubes in the foil affords very anisotropic mechanical and other physical properties. The nanotubes in direct contact with the quartz wall come first. They spend much more time in the hot zone of the reactor than the ones on the gray mat side of the ribbon. Being in direct contact with the quartz reactor, they are also heated to a higher temperature than the rest of the nanotubes in the foil. Finally, they suffer the load of the nanotubes accumulated above. Therefore, it is not surprising that the nanotubes in direct contact with the quartz wall collapse into flat wires (ribbons). A somewhat similar observation has been done before for WS_2 nanotubes, using a different growth procedure.[12] The growth of the sulfide-encapsulated oxide nanowhiskers is rather fast (<10 s)[6] and is likely to occur during the residence time of the nanoparticle in the vapor phase of the reactor. It is therefore very likely that the slow (60−120 min), diffusion-controlled conversion of the oxide core of the nanowhisker into closed tungsten−sulfide layers takes place when the nanotubes are already packed in the foil. Since the first encapsulating sulfide layer of the nanowhisker is formed in the gas phase, the chirality is imprinted in the nanotube already at this early stage of the growth.

Isolated WS_2 nanotubes and bundles thereof were also found mixed with a powder of fullerene-like nanoparticles in the center of the reactor in substantial amounts (a few grams per run). Figure 2a shows a low-magnification TEM of quite a typical bundle, consisting of three nanotubes. The 300-μm-long nanotubes are quite perfect in shape. It is very likely that much longer nanotubes

(12) Remskar, M.; Skraba, Z.; Regula, M.; Ballif, C.; Sanjinés, R.; Lévy, F. *Adv. Mater.* **1998**, *10*, 246.

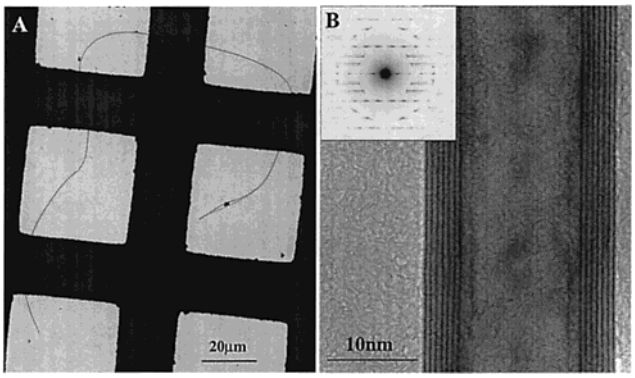

Figure 2. (a) A bundle of three very long WS_2 nanotubes; (b) high-resolution image of a WS_2 nanotube and its electron diffraction (inset) showing the helicity of the nanotube.

exist in the ribbons and in the bundles; however, it was not possible to separate them for analysis without damaging their integrity. Figure 2b shows a large-magnification image of a typical nanotube and its electron diffraction (ED) pattern. The flawless structure of the nanotube can be appreciated from the image, while the helicity of the nanotube is measured from the ED pattern.[13] Table 1 summarizes the data for a representative series of nanotubes. Achiral (zigzag or armchair) nanotubes have not been found in this study. The ED pattern nevertheless suggests that the nanotubes deviate only slightly from a zigzag arrangement. Tilting the nanotube in various angles in the TEM revealed that such isolated nanotubes are perfectly circular. This is to be contrasted with the nanotubes in the ribbon where distortion of part of the nanotubes was obvious (vide ultra).

Table 1. A Few Parameters Characterizing the Synthesized WS_2 Nanotubes

example	number of shells	helicity angle (deg)
1	8	7.5
2	5	6
3	7	4.5−11[a]
4	13	8.5

[a] This nanotube seems to be multihelical; arcs are observed instead of spots.

The growth mechanism of WS_2 nanotubes from oxide precursors has been discussed in some detail.[6,7] WO_3 whiskers have been studied and their growth mechanism elucidated (see for example refs 14 and 15). The key point here is the ability to control the elongation of the partially reduced oxide nanowhiskers, most particularly, the $W_{18}O_{49}$ phase, concomitantly with a mild sulfidization process of the outer surface of the growing oxide nanowhisker. This combination of concerted reactions, that is, elongation, reduction, and sulfidization, allows one to grow long and quite narrow and uniform WS_2 nanotubes in large amounts and in quite good purity.

Acknowledgment. We are grateful to A. Zak for the assistnace with the SEM anaysis. Prof. G. Seifert (Dresden) provided the scheme for the zigzag nanotube presented in the Table of Contents. This work was supported by the Israel Science Foundation, Israel Academy of Sciences (Bikura), and Israeli Ministry of Science (Tashtiot).

CM010630F

(13) Margulis, L.; Dluzewski, P.; Feldman, Y.; Tenne, R. *J. Microsc.* **1996**, *181*, 68.

(14) Sarin, V. K. *J. Mater. Sci.* **1975**, *10*, 593.

(15) Hashimoto, H.; Kumao, A.; Eto, T.; Fujiwara, K. *J. Cryst. Growth* **1970**, *7*, 113.